

Showcasing collaborative research by the Jordanian CO<sub>2</sub> team (JCO<sub>2</sub>T), represented by A. K. Qaroush (The University of Jordan, Jordan), K. I. Assaf (Jacobs University Bremen, Germany) and A. F. Eftaiha (The Hashemite University, Jordan)

#### Inedible saccharides: a platform for CO<sub>2</sub> capturing

Abundant, cost-effective, inedible saccharides represent potential candidates that can be exploited as green sorbents for CO<sub>2</sub> capturing. The efforts of the scientific community on using a wide spectrum of saccharides including cyclodextrins, chitin, chitosan and cellulose to capture CO<sub>2</sub> through physi- and chemisorption via dry and wet scrubbing applications are highlighted. The usage of oligomers, functionalisation of polymers, passing of “supramolecular chemisorption” convention and introduction of a Green tax are also suggested to mitigate CO<sub>2</sub>.

#### As featured in:



See Abdussalam K. Qaroush, Khaleel I. Assaf, Ala'a F. Eftaiha *et al.*, *Chem. Sci.*, 2018, 9, 1088.



[rsc.li/chemical-science](http://rsc.li/chemical-science)

Registered charity number: 207890



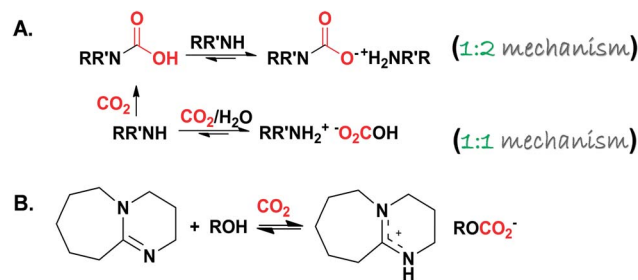


Following the seventh principle of green chemistry, our group established “renewables for renewables approach” which offers an eco-friendly platform to resolve environmental problems using renewable, inedible polymeric feedstocks for CO<sub>2</sub> capturing to promote future development benefiting from their environmental and economic impacts over petroleum-based feedstocks. Examples of renewable feedstocks include, but are not limited to, cellulose, cyclodextrin, chitin and chitosan (chemical structures are shown in Scheme 2).<sup>18–20</sup> A major inherent obstacle that hinders the use and processing of cellulose and chitin, despite their abundance in nature, is the limited solubility in common solvents,<sup>21,22</sup> which represents a significant technical challenge for both academic and sectors that demand the implementation of alternative greener strategies<sup>23,24</sup> other than those reported in the affiliated literature associated with dissolution and activation.<sup>25</sup>

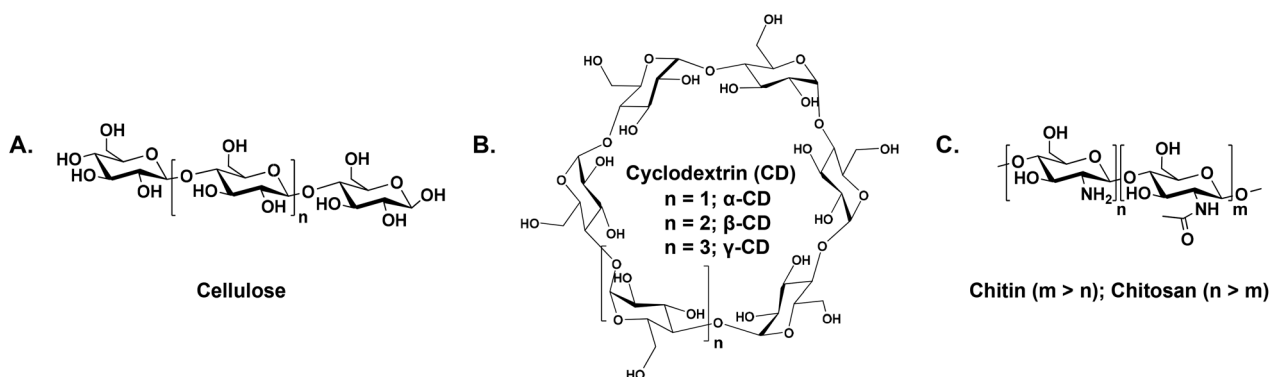
The fundamental aspects of liquid or solution based sorbents (typically utilised in the most mature capture technology) control the overall process in terms of sorption efficiency and kinetics together with regeneration.<sup>26</sup> It is expected that CO<sub>2</sub> is absorbed into the condensed phase in the low viscosity regimes, while it adsorbs at the surface of the sorbing material when the mass transfer is restricted to the bulk for high viscosity sorbents. Regarding the mechanism of action, when physical dissolution or physisorption is the prevailing mechanism, the uptake kinetics is expected to be slow and the desorption process is less energy demanding due to the weak, non-bonding interactive forces. If chemisorption is the dominant mechanism, the carbonation reaction is anticipated to be rapid and accompanied by a large energy requirement to regenerate the sequestered species. Chemisorption is accomplished *via* two different pathways: the first one is CO<sub>2</sub> capturing *via* “amine scrubbing” through the formation of carbamic acid/carbamate (RR'NH-CO<sub>2</sub><sup>-</sup> +NH<sub>2</sub>-RR') following a 1 : 1/1 : 2 reaction mechanism, respectively,<sup>27,28</sup> in which the nucleophilic attack over CO<sub>2</sub> by the amine nitrogen results in the formation of carbamic acid, which reacts with a second mole of amine (sacrificial base) to produce the carbamate salt. In the presence of water, a 1 : 1 reaction pathway takes place resulting in the formation of a bicarbonate (RR'NH<sub>2</sub><sup>+</sup> -O<sub>2</sub>COH)

zwitterionic adduct.<sup>29–31</sup> It is noteworthy that this pathway is followed when a benzylic amine (*o*, *m*, *p*-xylylenediamines) is used.<sup>32</sup> The proposed chemical reaction between amines and CO<sub>2</sub> is summarized in Scheme 3A. Similarly to conventional amine scrubbing agents, task-specific ionic liquids (TSILs and amine-functionalized ILs, Scheme 1B) form carbamate salts when exposed to CO<sub>2</sub>. Although TSILs have several merits over MEA aqueous solution in terms of lower CO<sub>2</sub> binding energies, milder regeneration conditions and higher capture capacities, they are not commercially available as MEA<sup>33</sup> (commercial sources of MEA (≥98%) list the retail price at \$25–\$40 per kilogram<sup>34,35</sup>). TSILs suffer from a huge increase in viscosity when loaded with CO<sub>2</sub> due to the hydrogen bonding (H-bonding) network between the carbamate and ammonium counterparts. This could be overcome by following different strategies such as incorporating an aprotic heterocyclic anion<sup>36</sup> or mixing TSILs with low-viscosity solvents<sup>37</sup> (more reviews regarding using TSILs for capturing CO<sub>2</sub> can be found elsewhere<sup>33,38</sup>).

The second pathway results in the formation of an inorganic or organic carbonate (M<sub>2</sub>(CO<sub>3</sub>)<sub>x</sub>, M<sup>+x</sup>: a metal cation, and ROCO<sub>2</sub><sup>-</sup>, respectively) following a 1 : 1 reaction mechanism. Aside from M<sub>2</sub>(CO<sub>3</sub>)<sub>x</sub>, the formation of ROCO<sub>2</sub><sup>-</sup> by activating alcohols to react with CO<sub>2</sub> was reported in the literature by two



Scheme 3 (A) Proposed chemisorption of CO<sub>2</sub> by amine based substrates (primary and secondary, the general formula is given for the secondary for clarification) through the formation of RR'N-CO<sub>2</sub><sup>-</sup> +NH<sub>2</sub>-R'R and RR'NH<sub>2</sub><sup>+</sup> -O<sub>2</sub>COH in the absence and presence of water, respectively. (B) The reversible reaction between an alcohol (ROH) and 1,8-diazabicyclo-[5.4.0]-undec-7-ene (DBU) in the presence of CO<sub>2</sub>.



Scheme 2 The chemical structures of (A) cellulose, (B) cyclodextrins, and (C) chitin ( $m > n$ ) and chitosan ( $m < n$ ).



research groups. Firstly, Jessop and co-workers<sup>39,40</sup> devised CO<sub>2</sub> binding organic liquids (CO<sub>2</sub>BOLs) which comprised of anhydrous alcohol and a superbase (SB). An example reaction is shown in Scheme 3B. The high volatility associated with CO<sub>2</sub>-BOLs and the hardship of drying/handling, together with the high corrosive character, paved the way toward single component CO<sub>2</sub>BOLs<sup>17</sup> (Scheme 1C) that unfortunately exhibited high viscosity upon chemisorption. Afterwards, Sir J. F. Stoddart's group<sup>41–44</sup> reported that the hydroxyl groups located at the rim of  $\gamma$ -cyclodextrin-based metal-organic frameworks (CD-MOFs) are capable of reacting with CO<sub>2</sub> reversibly to form a metal-stabilized organic alkyl-carbonate (a detailed discussion is provided, *vide infra*).

Most of the literature reports focus on the capturing process highlighting the high-energy penalty associated with the regeneration of conventional aqueous amine solvents in comparison with alcohol/SB binary mixtures that suffer from high volatility and corrosiveness, which makes the use of aprotic solvents a reasonable alternative to increase the efficiency of carbon dioxide desorption as they have a lower heat capacity than aqueous based sorbents and a higher vapor pressure as introduced by Park and colleagues,<sup>45</sup> and followed-up by our research group.<sup>28,46,47</sup> As a matter of fact, the solvation of ions is of great importance when forming CO<sub>2</sub> adducts from neutral solutions. Accordingly, cations are well solvated in polar aprotic solvents, while anions are poorly solvated, therefore, this might favour a shift in the equilibrium towards the neutral species and, consequently, pK<sub>a</sub> values greater than that formed while working in aqueous solutions.<sup>45</sup>

In this minireview, recent advances on the sorption of CO<sub>2</sub> by inedible saccharides is discussed as follows: (1) a review of the reversible reaction between cellulose and CO<sub>2</sub>, and the subsequent dissolution and regeneration; (2) the capture and storage of CO<sub>2</sub> by cyclodextrins; (3) the chemisorption of CO<sub>2</sub> by chitin and chitosan using ILs, oligomers and nanoparticles; and (4) CO<sub>2</sub> capturing using functionalised cellulosic materials. We conclude with the challenges and future outlooks of exploiting bio-renewables to be implemented in the area of CCS research.

## Cellulose

Cellulose, a low-value agricultural by-product, is the most naturally occurring biopolymer, with a production capacity of ca. 180 billion tons per annum by plants.<sup>48,49</sup> It is a linear polymer consisting of  $\beta$ -(1,4)-linked glucopyranose units (Scheme 2A). It is characterized by strong inter- and intramolecular H-bonding which play a major role in its structural stability, chemical properties and resistance to enzymatic hydrolysis. One major obstacle that hinders the effective utilisation of cellulose is its insolubility in conventional solvents due to the semicrystalline structure.<sup>21</sup> Over the past few years, several solvent systems for the dissolution of cellulose have been reported<sup>50–54</sup> that suffered from serious drawbacks such as corrosiveness, high cost, and reduced dissolution capacity in the presence of polar solvents as well as recycling and purification difficulties which required alternative eco-friendly

approaches for cellulose processing such as the use of pressurised CO<sub>2</sub> to precipitate cellulose from ILs.<sup>55–59</sup>

Following the concept of switchable solvents, Jérôme and co-workers<sup>60</sup> reported on the dissolution of microcrystalline cellulose (MCC) suspended in a mixture of dimethyl sulfoxide (DMSO) and 1,5-diazabicyclo[4.3.0]non-5-ene (DBN) upon bubbling CO<sub>2</sub>. In the presence of a SB, the primary hydroxyl groups along the cellulose backbone reacted with CO<sub>2</sub> resulting in the formation of carbonate species. The process could be reversed by heating the solution at 30 °C under vacuum, by which the cellulose was precipitated (Fig. 1). After exposing this precipitate to CO<sub>2</sub>, the cellulose was dissolved again which highlighted the reversibility of the system. It is noteworthy that the use of weak bases was not efficient to dissolve cellulose under the investigated conditions, as they were incapable of activating the hydroxyl groups.

Another example of a reaction between cellulose and CO<sub>2</sub> in the presence of a SB (namely 1,8-diazabicyclo-[5.4.0]-undec-7-ene, DBU), yielding [DBUH]<sup>+</sup>[cellulose-OCO<sub>2</sub>]<sup>-</sup>, was reported by Yang *et al.*<sup>61</sup> The reaction allowed a successful dissolution of the cellulose pulp, and subsequently allowed its modification into cellulose acetate using acetic anhydride (Scheme 4A). Mu and co-workers<sup>62</sup> monitored the formation of the aforementioned adduct *via in situ* infrared spectroscopy. The formed carbonated cellulose underwent a chemical reaction with a silane-based reagent (TEOS: tetraethyl orthosilicate) which provided a green method for the preparation of a superhydrophobic nanocoated material (Scheme 4B). Moreover, a cellulose-graft-poly(L-lactide) copolymer was synthesized, exploiting the reversible character of the aforementioned reaction. DBU had a dual action in cellulose dissolution with its role as an organocatalyst for the subsequent ring-opening polymerization process (Scheme 4C).<sup>63</sup>

Once again, Mu's research group<sup>64</sup> reported a detailed study of the dissolution process to understand the mechanism for the formation of a MCC carbonated/SB adduct in DMSO upon bubbling CO<sub>2</sub>. It was found that DMSO helped in the dissociation of the adduct into free ions by balancing the concentration of the ions and the number of hydrogen bonds. In this context, density functional theory (DFT) calculations revealed multiple interactions between the protonated base and the carbonated cellulose. Very recently, the chemisorption of CO<sub>2</sub> onto cellulose in aqueous NaOH solution in the absence of a SB has been

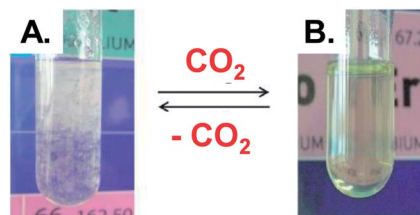
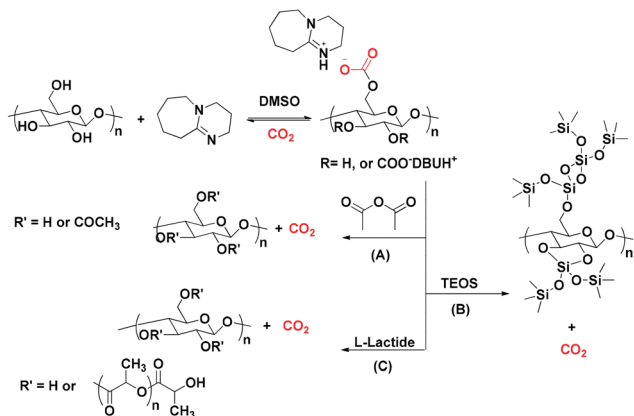


Fig. 1 Photographs of (A) a suspension of MCC in DMSO containing 9 wt% of DBN and (B) a transparent, viscous solution with a maximum concentration of 6 wt% cellulose, obtained after exposing the suspension at 40 °C to 2 bar of CO<sub>2</sub> for 1 hour. Reprinted with permission from ref. 60.





Scheme 4 The versatility of cellulose in several applications upon activation through its reaction with CO<sub>2</sub> in the presence of DBU.

reported by Gunnarsson *et al.*<sup>65</sup> and confirmed using both nuclear magnetic resonance (NMR) and attenuated total reflectance Fourier transform infrared spectroscopy (ATR-FTIR). The reversibility of the reaction was achieved by the addition of water. In addition, treating cellulose with NaOH and CO<sub>2</sub> in dimethylacetamide (DMAc) resulted in the formation of carbonated cellulose.<sup>66</sup> FTIR spectroscopy supported the introduction of the new functionality of cellulose *via* the existence of a band at 1593 cm<sup>-1</sup>, as well as a decrease in intensity of the peak associated with hydrogen bonded hydroxyl groups.<sup>66</sup>

The use of 1,1,3,3-tetramethylguanidine (TMG), in combination with an alcohol dissolved in DMSO revealed a new switchable solvent system that was capable of dissolving cellulose after exposure to CO<sub>2</sub>.<sup>67</sup> The authors attributed the dissolution phenomenon to the formation of a guanidinium alkylcarbonate salt, as identified by both <sup>13</sup>C NMR (the emergence of a new peak at 159.2 ppm) and *in situ* FTIR (newly formed asymmetric and symmetric carbonyl stretching bands at 1663 and 1410 cm<sup>-1</sup>, respectively). The dissolution of cellulose was alcohol dependent. In the case of ethylene glycol, a fully transparent cellulose solution was observed, allowing for a maximum de-crystallization up to 10 wt% concentration with high stability. In accordance with a previous report,<sup>60</sup> no dissolution of cellulose was observed when weak bases (pK<sub>a</sub> < 12) were utilised.<sup>67</sup> In the same context, Nanta *et al.*<sup>68</sup> applied a similar switchable solution consisting of DBU and ethylene glycol in DMSO under high-pressure carbon dioxide to facilitate the dissolution and modification of cellulose derived from cassava pulp waste.

### Cyclodextrin

Cyclodextrins (CDs, Scheme 2B) are a class of naturally occurring cyclic oligosaccharide that are obtained *via* the enzymatic degradation of starch. They consist of  $\alpha$ -D-glucopyranose units linked *via*  $\alpha$ -1,4 linkages in a truncated cone shape, which has a hydrophobic cavity and a hydrophilic outer surface. While the secondary hydroxyl groups are located on the wider rim of the cone, the primary counterparts are on the narrower one.<sup>69</sup> The supramolecular chemistry of CDs makes them useful for a wide

range of applications in different fields such as pharmacy, food, medicine, the environment and engineering.<sup>70</sup>

Sir J. F. Stoddart and his research group exploited the symmetry of  $\gamma$ -CD to synthesize nanoporous materials, which is a prerequisite to induce crystallization upon coordinating the macrocyclic motif to a metal centre, with surface areas of  $\sim 1200$  m<sup>2</sup> g<sup>-1</sup> under mild conditions. It has been reported that  $\gamma$ -CD tends to assemble into crystalline MOFs in the presence of alkali metal salts, and are grown from the vapour diffusion of methanol (MeOH).<sup>71,72</sup> Among all investigated MOFs, CD-MOF-2, comprised of  $\gamma$ -CD and rubidium cations (Rb<sup>+</sup>), showed an outstanding stability after the removal of the solvent compared with other cubic CD-MOFs prepared from potassium (K, CD-MOF-1) and caesium (Cs, CD-MOF-3) salts,<sup>73</sup> which makes it useful for subsequent investigations as a CO<sub>2</sub> sorbent.<sup>41-43</sup> Fig. 2A and B show ball-and-stick and space filling representations of CD-MOF-2, respectively.

The chemisorption of CO<sub>2</sub> by CD-MOF-2 was proved using cross-polarization magic-angle-spinning (CP/MAS) <sup>13</sup>C NMR spectroscopy through the emergence of a new peak at 158 ppm that was attributed to the formation of the alkyl carbonic acid based CD-MOF, which was further supported calorimetrically. As shown in Fig. 2C, the addition of methyl red to CD-MOF-2 crystals resulted in a yellow colour due to the basic environment within the framework. Upon exposure to CO<sub>2</sub>, the yellow

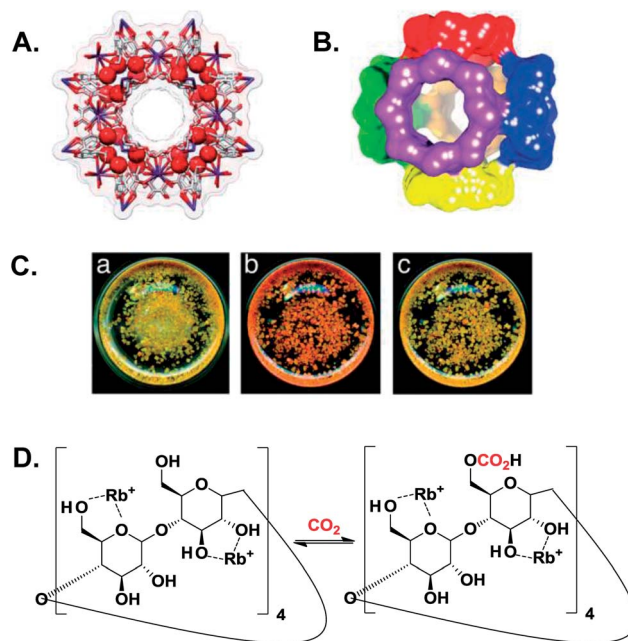


Fig. 2 (A) A ball-and-stick view of a cubic array made of ( $\gamma$ -CD)<sub>6</sub> units coordinated to 24 Rb<sup>+</sup> (red spheres) through the ring oxygen atoms of the secondary and primary hydroxyl groups. (B) A space-filling depiction of six ( $\gamma$ -CD)<sub>6</sub> units that link together in a body-centered cubic extended framework. (C) Photographs of CD-MOF-2 incorporating methyl red before (a) and after (b) exposure to CO<sub>2</sub>. Removal of the CO<sub>2</sub> atmosphere restored the colour back to yellow (c). A–C are adapted with permission from ref. 41. (D) A proposed carbonation reaction of activated CD-MOF-2 at the less reactive primary hydroxyl groups, where the free hydroxyls act as nucleophiles to attack CO<sub>2</sub>.<sup>41</sup>



colour turned red which was attributed to the formation of carbonic acid throughout the framework, and returned back to yellow after the removal of CO<sub>2</sub>. It was noteworthy that the CP/MAS spectra of iso-structural CD-MOFs prepared from rubidium fluoride or potassium benzoate (rather than rubidium hydroxide as in the case of CD-MOF-2) revealed identical resonances at 158 ppm, which discard the importance of the hydroxide anion in facilitating chemisorption in comparison with weaker nucleophiles such as fluoride and benzoate anions.<sup>41</sup> The same conclusion was obtained from the substantial difference between the adsorption enthalpy on CD-MOF-2 at near-zero coverage and an analogous acid–base reaction that involved a significant concentration of free hydroxide anions (OH<sup>−</sup>), which suggested that the adsorption took place through the alcoholic functional groups, rather than the interstitial OH<sup>−</sup> (*vide infra*).<sup>42</sup> Adsorption isotherms indicated that chemisorption was the dominant mechanism between 0 and 25 °C with a sorption capacity of ~23 cm<sup>3</sup> CO<sub>2</sub> per g sorbent.<sup>41</sup>

Mechanistic insight into the adsorption of CO<sub>2</sub> on CD-MOF-2 was obtained using calorimetric measurements. The differential enthalpy of the carbonation reaction confirmed that the chemisorption followed two distinct patterns. Firstly, at near-zero coverage with a highly exothermic reaction (−113.5 kJ mol<sup>−1</sup> CO<sub>2</sub>) *via* the most reactive primary hydroxyl groups, followed by a milder reaction (−65.4 kJ mol<sup>−1</sup> CO<sub>2</sub>) through the less reactive primary and secondary hydroxyl groups at a surface coverage between 0.1 and 0.3. At a higher surface coverage (>0.4), physisorption is the dominant adsorption mechanism with a differential enthalpy of −40.1 kJ mol<sup>−1</sup> CO<sub>2</sub>.<sup>42</sup> In our consensus regarding the reaction reversibility, there was unsurprising inconsistency between the results obtained from the isothermal gas uptake and the calorimetric data. The former designated a reversible chemical fixation of CO<sub>2</sub>,<sup>41</sup> the difference between the enthalpy of adsorption at near-zero coverage and the subsequent adsorption cycles indicated an irreversible binding character between the most reactive primary hydroxyl groups and CO<sub>2</sub>, followed by a reversible binding on the less reactive hydroxyls together with the physisorbed CO<sub>2</sub>.<sup>42</sup> The carbonation reaction of CD-MOF-2 is shown in Fig. 2D.<sup>74</sup>

The challenge in synthesizing CD-MOFs with cations other than K<sup>+</sup>, Rb<sup>+</sup> and Cs<sup>+</sup>, is the inability to obtain porous, crystalline frameworks. Very recently, Patel *et al.*<sup>44</sup> demonstrated the partial substitution of K<sup>+</sup> with Li<sup>+</sup> through co-crystallizing KOH and LiOH with γ-CD. As shown in Table 1, the most stable Li/K-CD-MOF with the highest Li<sup>+</sup>:K<sup>+</sup> ratio (0.61:1.18) had a comparable Brunauer–Emmett–Teller (BET) surface area and a characteristic better sorption in comparison with those obtained for other iso-structural CD-MOFs.

The reversible chemisorption of CO<sub>2</sub> by CD-MOF-2 was utilised for the electrochemical sensing of CO<sub>2</sub>. Unexpectedly, it has been reported that CD-MOF-2 (either as a pristine powder or pellet<sup>76</sup>) displayed a ~550-fold decrease in ionic conductivity upon exposure to CO<sub>2</sub> for 5 minutes in the presence of MeOH or *n*-hexane, although carbonic acid is relatively more acidic than primary alcohols. This was attributed to the sealing of the β-

windows (small triangular-shape voids of diameter 4.2 Å, Fig. 3) of the [(Rb<sup>+</sup>)<sub>4</sub>(γ-CD)]<sub>6</sub> cubic cages after the carbonation reaction, where the reactive primary hydroxyl groups are located, thus reducing the mass transfer of intermediate molecules. The sensor reusability was tested by measuring the change in conductivity of a CD-MOF-2 pellet following sequential CO<sub>2</sub>-sorption and desorption (by heating at ~80 °C for several cycles). It was noteworthy that the conductivity change was higher at low CO<sub>2</sub> concentration (less than 20% in the presence of N<sub>2</sub> gas).<sup>40</sup>

Aside from CD-MOFs, it has been reported that the inclusion complex of 1:1 β-CD and aniline (CD–aniline) in association with residual water molecules inside the CD cavity, chemisorbed CO<sub>2</sub> with a sorption efficiency of 0.69 mmol of CO<sub>2</sub> per g sorbent through the formation of bicarbonate according to the following reaction: C<sub>6</sub>H<sub>5</sub>NH<sub>2</sub> + CO<sub>2</sub> + H<sub>2</sub>O ⇌ C<sub>6</sub>H<sub>5</sub>NH<sub>3</sub><sup>+</sup> HCO<sub>3</sub><sup>−</sup>. The sorption capacity was decreased by 37% when the sorbent was heated to 100 °C under vacuum, which emphasized the importance of the water molecules to the sequestration process.<sup>75</sup> Although the performance characteristics of the CD–aniline complex were much lower than the corresponding CD-MOFs, it sorbed 0.85 mol CO<sub>2</sub> per mol nitrogen (N) in comparison with the amine efficiency of 0.5 mol CO<sub>2</sub> per mol N following a 2:1 sorption mechanism under dry conditions, which was unlikely to take place in the case of the explored inclusion complex. Unlike CD-MOFs (*vide supra*), the sorption capacity of the amorphous CD–aniline complex (obtained upon grinding) was almost similar to the as-synthesised crystalline material.

Han and co-workers<sup>76</sup> reported the facile and elegant synthesis of CD-based microporous carbon (CDPC) using acid catalysed solvothermal carbonization at 180 °C. The obtained materials were regular spheres with diameters between 300 and 800 nm, BET surface areas ranging from 600 to 700 m<sup>2</sup> g<sup>−1</sup> and high content of oxygen-containing functional groups, such as carboxyl, carbonyl, and hydroxyl as inferred from FTIR and <sup>13</sup>C CP/MAS spectra. As shown in Table 1, the CO<sub>2</sub> gravimetric uptake of α-, β- and γ-CDPC measured at 0 °C and 1.0 bar were between 2.8 and 3.5 mmol CO<sub>2</sub> per g sorbent. Similarly, it has been reported that grafting β-CD with sulfonic acid functional groups (−SO<sub>3</sub>H) led to the formation of a porous structure (CD–SO<sub>3</sub>H) with a low oxygen content due to dehydration, which was able to physisorb CO<sub>2</sub> 30 times more than β-CD at the same investigated conditions (1.2 of the former against 0.04 mmol CO<sub>2</sub> per g sorbent of β-CD) with high selectivity over O<sub>2</sub>, N<sub>2</sub> and CH<sub>4</sub>, which makes it a potential candidate for CO<sub>2</sub> separation from flue gas.<sup>77</sup>

Turning to wet scrubbing applications, the hydroxyl groups of the CD macrocycle should be activated to become susceptible to nucleophilic attack prior the exposure to CO<sub>2</sub>. It has been reported that a mixture of β-CD and an organic SB, namely DBU, was able to fix CO<sub>2</sub> chemically as an amidinium alkylcarbonate. Due to viscosity issues, the ratio (in equivalents) of β-CD:DBU was kept at 0.5:1 throughout the work. The carbonation reaction was followed by <sup>1</sup>H and <sup>13</sup>C NMR together with FTIR spectroscopy, following the peaks associated with the quaternary carbon of DBU. The relatively low uptake of CO<sub>2</sub> (1.8 wt%)



Table 1 Surface area, mechanism of sorption and sorption capacity of different solid CD-based sorbents

Sorbent	BET surface area (m <sup>2</sup> g <sup>-1</sup> sorbent)	Sorption mechanism	Sorption capacity (mmol CO <sub>2</sub> per g sorbent)	
			0 °C	25 °C
CD-MOF-1	1145 (ref. 44) (1320 (ref. 71))	Chemi & physisorption	4.2 (ref. 44)	3.0 (ref. 44)
CD-MOF-2	1110 (ref. 71)		1.7 (ref. 44)	1.4 (ref. 44)
Li/K-CD-MOF	1205 (ref. 44)		4.5 (ref. 44)	3.1 (ref. 44)
CD-aniline	NA	Chemisorption		0.69 <sup>c</sup> (ref. 75)
α-CDPC	703 (ref. 76)		Physisorption	3.3 (ref. 76)
β-CDPC	699 (ref. 76)		2.9 (ref. 76)	NA
γ-CDPC	678 (ref. 76)		2.8 (ref. 76)	NA
CD-SO <sub>3</sub> H	211 (ref. 77)		NA	1.2 <sup>a</sup> (ref. 77) 1.7 <sup>b</sup> (ref. 77)

<sup>a</sup> The uptake was measured at 1 bar. <sup>b</sup> The uptake was measured at 3 bar. <sup>c</sup> The CO<sub>2</sub> adsorption experiment was carried out at 30 °C.

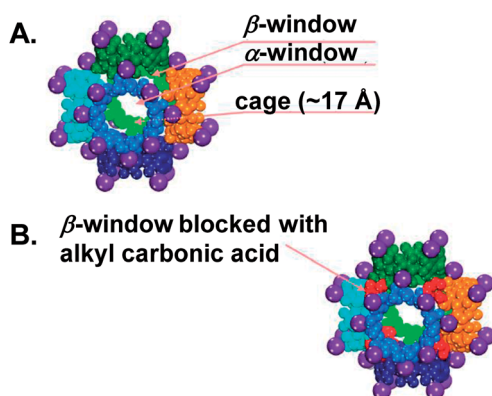


Fig. 3 A space-filling representation of [(Rb<sup>+</sup>)<sub>4</sub>(γ-CD)]<sub>6</sub> cubic cages. Purple spheres indicate Rb<sup>+</sup>; the sides of the cube (six-CD rings) are depicted in different colours. Adapted with permission from ref. 43.

was explained by the excessive use of the SB together with the inefficient stirring during the synthesis of the sequestered species. Notably, the sorption capacity was 7.9 wt% in the case of glucose : DBU mixture.<sup>78</sup>

### Chitin and chitosan

Among the various, spread polysaccharides, amine containing sugars, in which the –OH group at C-2 of the hexose monomeric unit is replaced by –NH<sub>2</sub>, are the main component of chitin (Scheme 2C, *m* > 50%), which is mainly found in crustaceans, insects, molluscs, bacteria and fungi. The insolubility of chitin in common solvents represents a considerable barrier that confronts its employment in various fields. In the early eighties of the last century, Austin<sup>79</sup> explored the solubility of a chitin-lithium chloride (LiCl) complex in several amide solvents such as DMAc and *N*-methyl-2-pyrrolidone (NMP), followed by several attempts to dissolve chitin using salts and acids (for more details, see the review by Rinaudo<sup>22</sup>). Deacetylation of chitin either enzymatically or under alkaline conditions<sup>80</sup> results in chitosan (Scheme 2C, *n* > 50%). The solubility of chitosan in aqueous acidic media is dependent on several structural parameters such as the degree of deacetylation, the distribution

of the acetyl-groups along the polymer backbone and the molar mass.

In 2006, Zhang and co-workers<sup>81</sup> reported on the use of ILs, namely 1-butyl-3-methyl-imidazolium chloride (Bmim)Cl, as an alternative solvent for chitin and chitosan due to its ability to break down the polymer crystallinity under mild conditions as inferred from wide-angle X-ray diffraction (WAXD) measurements. Interestingly, both chitin and chitosan were recovered from the IL solution using methanol or water. The sorption efficiency of 10 wt% solutions of chitosan/IL and chitin/IL were measured gravimetrically using a microbalance at 30 °C and 1 atm CO<sub>2</sub> pressure. Results indicated that the efficiency of the former was 8.1% compared to 3.8% for the latter. Although no spectroscopic evidence for chemisorption was provided, the authors justified the higher sorption capacity of the chitosan-based solution by the chemical fixation of CO<sub>2</sub> due to the presence of free amine groups which are either blocked or presented in a lower fraction in the case of chitin. Regarding regeneration, it was reported that heating the chitosan/IL solution at 100 °C for 30 minutes reduced the sorption efficiency to 1.4%, afterwards the IL solution can be used for subsequent capture/release cycles.

The sorption capacity measurements performed by Mu's research group<sup>82</sup> using 6 wt% of chitosan or chitin dissolved in 1-butyl-3-methylimidazolium acetate (Bmim)OAc were consistent with those reported previously by Zhang's group.<sup>81</sup> The values obtained using thermogravimetric analysis (TGA) were 6.7 and 3.5% for chitosan and chitin, respectively, whereas it was 1.3% for neat (Bmim)OAc. The almost doubled capacity of the former suggested that chemisorption was the main mechanism for CO<sub>2</sub> capturing through carbamate formation in the case of chitosan, while physical dissolution was responsible for the capturing in the case of chitin. The chemisorption was proved using ATR-FTIR spectroscopy through the disappearance of the peak at 1680 cm<sup>-1</sup> which belongs to the bending mode of N–H, the appearance of a new peak centred at 1652 cm<sup>-1</sup> ascribed to –N–C(O)– amide moiety of the carbamate ion. The sequestered species was regenerated under 1 atm N<sub>2</sub> at 80 °C. The ability of the compressed CO<sub>2</sub> to act as an anti-solvent<sup>56,83</sup> was exploited to precipitate chitosan through the reaction between CO<sub>2</sub> and the acetate-based ILs to end up with





the formation of a carboxylate zwitterionic dimer that changes the hydrogen-bonding properties of the IL as inferred from the measurements of the solvatochromic parameters.

Recently, Wasserscheid and co-workers introduced a new type of immobilized IL by encapsulating IL<sup>84</sup> or ionogel droplets<sup>85</sup> (chitosan dissolved in IL and diluted with acetonitrile (ACN)) in fumed silica forming a free-flowing IL (ionogel)-in-air powder or inverse supported ionic liquid phase (SILP) material (Fig. 4) after evaporating the ACN. The key advantages of the inverse SILP is the high ratio of IL (ionogel) to the nanoporous material together with relatively short gas diffusion distances.

The gravimetric absorption capacity of the inverse SILP made of 40 wt% IL or ionogel (with 5 wt% of chitosan) and 60 wt% silica measured at 1 bar and 40 °C ranged between 0.1 and 0.8 mmol CO<sub>2</sub> per g sorbent. The results indicated that the CO<sub>2</sub> uptake was increased when an IL with a weakly basic anion such as chloride or 2-methoxyethyl methylphosphonate were used due to the extra carbamation reaction provided by chitosan together with the enhanced solubility of CO<sub>2</sub> in an ionogel compared with the corresponding IL. However, employing a more basic anion such as acetate obstructed the chemistry of sorption by chitosan due to an acidic side product obtained from the carbonation reaction of the IL itself. In comparison with neat chitosan powder, the absorption capacity calculated based on the number of amino groups present in chitosan was improved by 10 times in the inverse SILP. The low absorption efficiency of the neat chitosan was attributed to the restriction of the carbamation reaction at the interface of the powder.

Amine-functionalized porous materials represent an alternative technology for CO<sub>2</sub> capturing.<sup>12</sup> Chitosan represents a promising alternative for mesoporous silica in the quest to find eco-friendly and low-cost materials to be used as an amine support. Fujiki and Yogo<sup>86,87</sup> reported on porous chitosan beads impregnated with polyethyleneimine (PEI) working under both dry and humid conditions with CO<sub>2</sub> adsorption capacity of 2.38 and 3.61 mmol per g sorbent, respectively, at 15 kPa of CO<sub>2</sub> and 66 °C through the formation of ammonium carbamate as confirmed by *in situ* diffuse reflectance infrared Fourier

transform spectroscopy (DRIFTS). The enhanced CO<sub>2</sub> adsorption under wet conditions was explained by the swelling of the chitosan framework, thus exposing buried amino groups to CO<sub>2</sub>, which resulted in the formation of two adsorption states of CO<sub>2</sub> (whereas one state was recognised under dry conditions) as indicated by TGA measurements.

Although Zhang<sup>81</sup> opened new horizons for exploiting chitin for CO<sub>2</sub> capturing through physical dissolution, our research group published the first report on the chemisorption of CO<sub>2</sub> by an oligomeric chitin acetate (CA)/DMSO binary mixture.<sup>88,89</sup> The only functional groups along this oligomeric material available for the capturing process were the hydroxyl groups whereas the amino groups at C-2 of the amine pyranose rings were blocked either by protonation or acetylation. Herein, the use of DMSO was a prerequisite for the carbonation reaction to take place through the intermolecular hydrogen bonding between the polar aprotic solvent and primary hydroxyl group at C-6 of the pyranose ring which prompted the nucleophilic attack at CO<sub>2</sub> to form the organic alkyl-carbonate as follows:  $\text{RCH}_2\text{OH} + \text{CO}_2 \rightleftharpoons \text{RCH}_2\text{OCO}_2^- + \text{H}^+$ . The formation of the CO<sub>2</sub> sequestered species was confirmed using <sup>13</sup>C NMR and *in situ* ATR-FTIR spectroscopy, through the appearance of the benchmark chemical shift at *ca.* 157 ppm together with a peak centred at 1555 cm<sup>-1</sup> which was ascribed to the vibrational mode of the carbonate. Notably, glucosamine hydrochloride (the monomeric unit of the oligomer) showed no chemisorption upon bubbling CO<sub>2</sub>. The stability aspects of the organic carbonate adduct were understood using <sup>1</sup>H NMR spectroscopy and DFT calculations that indicated that the product was stabilized through non-bonding interactions, namely H-bonding and ionic interaction along the oligomer backbone. This indicated that the supramolecular stabilization was the driving force for the chemisorption, which was absent in the case of glucosamine hydrochloride. The CO<sub>2</sub> sorption uptake was measured volumetrically using *in situ* ATR-FTIR autoclave with a maximum capacity of 3.63 mmol CO<sub>2</sub> per g sorbent for a 10.0% (w/v) CA/DMSO solution. The decrease in the sorption capacity with increased concentration was attributed to the huge increase in viscosity at higher concentration of the oligosaccharide solution, which may have hindered the diffusion of CO<sub>2</sub> to the bulk of the solution.

To ultimately maximize the sorption capacity of CO<sub>2</sub>, while using bio-renewable and inedible materials, we moved our attention over oligomeric chitosan due to the presence of two potential active sites to interact with CO<sub>2</sub>, through the formation of carbonate and carbamate. In this context, our group reported on the use of a low molecular weight chitosan hydrochloride (CS·HCl) dissolved in DMSO for CO<sub>2</sub> sequestration.<sup>90</sup> Upon bubbling CO<sub>2</sub>, the formation of the organic carbonate adduct was consistent with the previously affiliated system and ascribed to the supramolecular chemisorption. *Ex situ* ATR-FTIR spectroscopy of the CS·HCl/NaOH/DMSO solution confirmed the formation of the other sequestered functionality, *viz.* ammonium carbamate, after bubbling CO<sub>2</sub>, through the appearance of the fingerprint frequency at 1709 cm<sup>-1</sup> which was further elucidated using <sup>1</sup>H-<sup>15</sup>N heteronuclear single quantum coherence (HSQC) NMR spectroscopy, with coupled cross-peaks

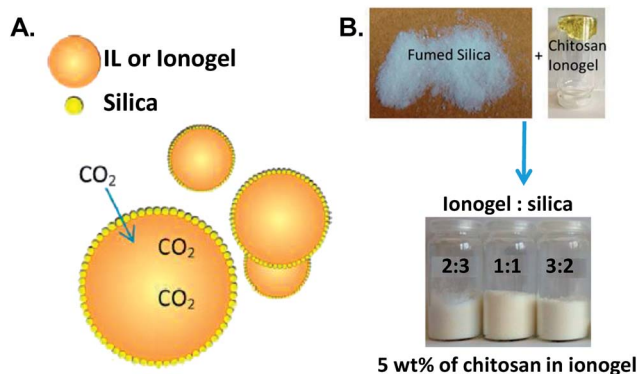


Fig. 4 (A) Depiction of an inverse SILP. (B) A photograph of inverse SILPs prepared from an ionogel comprised of 5 wt% chitosan dissolved in 1-ethyl-3-methylimidazolium acetate ([EMIM][OAc]) with different ionogel to silica ratios. Reprinted with permission from ref. 84 and 85.



at 6.8 (correlated to the ammonium counterpart chemical shift) and 84.7 ppm. The CO<sub>2</sub> uptake of the CS·HCl/NaOH/DMSO solution was quantified volumetrically using an *in situ* ATR-FTIR autoclave. A 10% (w/v) solution chemisorbed 1.60 mmol CO<sub>2</sub> per g sorbent. Remarkably, the formation of the carbonate was four times that of the carbamate, with faster kinetics for the latter as inferred from the sorption profiles. To our knowledge, this was the first organic carbamate-carbonate bond formation.

One of the major concerns regarding the greenness of DMSO was answered by measuring the biodegradability of the explored system. Following the guidelines of the International Organization for Standardization (ISO), the relatively fast degradation of chitosan dissolved in DMSO (80% in 33 days) provided clear-cut evidence for the absence of any tangible negative impact of using DMSO on the biodegradation of chitosan.

### Cellulose-based functionalized sorbent materials

The main uses of cellulose as an abundant biopolymer that functions as a mechanical support and in sustainable porous carbon-based materials, as well as for the preparation of hollow fibres as in membranes for the capturing of CO<sub>2</sub>, are reported in this section.

In 2011, Steinfeld and co-workers<sup>91</sup> reported a novel, eco-friendly, benign synthesis for an amine-based nanofibrillated cellulose (NFC) sorbent applicable for CO<sub>2</sub> capture from air using *N*-(2-aminoethyl)-3-aminopropylmethyldimethoxysilane (AEAPDMS). At 25 °C and after 12 h, 1.39 mmol CO<sub>2</sub> per g sorbent was sorbed with a relative humidity of 40% and 506 ppm of CO<sub>2</sub> concentration in air. The studied material showed persistent stability over 20 consecutive 2-hour adsorption/1-hour desorption cycles. The cyclic capacity of the resultant cycles gave 0.695 mmol CO<sub>2</sub> per g sorbent. Once again, as an augmentation to Steinfeld's<sup>92</sup> early work on NFC, the stability of amine-tethered-NFC for CO<sub>2</sub> capturing from air (400–530 ppm) under temperature–vacuum swing (TVS) conditions was tested 100 times at 30 °C and 60% humidity for adsorption, followed by desorption at 90 °C and 30 mbar. The average adsorption capacity under the applied conditions was 0.90 mmol CO<sub>2</sub> per g sorbent. Due to the presence of O<sub>2</sub>, the sorbent degraded at 90 °C, reducing its adsorption capacity by 30% (after 15 h and dew point of 22 °C). On the other hand, if moist CO<sub>2</sub> was introduced to the sample at the same applied conditions, no tangible loss in CO<sub>2</sub> adsorption capacity was recorded. Sevilla and Fuertes<sup>93</sup> reported on the utilisation of sustainable porous carbon materials that were prepared using the chemical activation of hydrothermally carbonized starch, cellulose and sawdust (one type of biomass) and further tested for capturing purposes. The activation process was carried out under both severe and mild conditions (KOH/precursor = 4 and 2, respectively, within a set of temperatures in the range of 600–800 °C). Samples obtained under mild activating conditions showed smaller pore sizes and surface areas than those materials obtained under harsher conditions. However, they exhibited the best capacity to store CO<sub>2</sub> which is equivalent to 4.8 mmol g<sup>-1</sup> (at 25 °C with KOH/precursor = 2 and activated at 600 °C). According to the authors, this was the highest value for any activated carbon. The

prepared materials showed fast adsorption kinetics and easy regeneration with good CO<sub>2</sub>/N<sub>2</sub> selectivity measured under equilibrium conditions ~5.4. Pacheco *et al.*<sup>94</sup> reported on the modification of an aminosilane-functionalized cellulosic polymer sorbent by the anhydrous grafting of *N*-(2-aminoethyl)-3-aminoisobutyldimethylmethoxysilane. The sorption capacity under dry conditions (5 atm, 308 K) was 1.46 mmol per g sorbent with an amine loading of 5.18 mmol amine(nitrogen) per g sorbent. Working under humid conditions facilitated the uptake up to 12% at 1 atm. Moreover, Koros and co-workers<sup>95</sup> reported on the use of another type of cellulose acetate fibres that were aminated with (*N*-(2-aminoethyl)-3-aminoisobutyldimethylmethoxysilane). Using a pressure decay apparatus, the CO<sub>2</sub> sorption capacity was a bit low (0.73 mmol CO<sub>2</sub> per g sorbent at 1 atm).

Heo and Park<sup>96</sup> reported on the preparation of ultra-microporous carbons from cellulose fibres by means of physical activation at different temperatures. Using steam, the physical activation influenced the development of new micropores for CO<sub>2</sub> storage. The adsorption capacity for the synthesized materials was 3.776 mmol CO<sub>2</sub> per g sorbent at 298 K and 1 atm with a good CO<sub>2</sub>/N<sub>2</sub> selectivity of 47.1. The studied material was regenerated 10 times after repeated sorption/desorption cycles. Their work showed the importance of carbon materials with good adsorption abilities without the need for chemical activation. In 2016, Einloft and co-workers<sup>97</sup> reported on the use of rice-husk cellulose-supported ionic liquids for the capture of CO<sub>2</sub>. The uptake experiments were gravimetric with optimal values for cellulose-modified tetrabutylammonium (CL-TBA) of 44 and 71 mg CO<sub>2</sub> per g sorbent at 25 °C and 0.1 and 3 MPa, respectively.

Organoclays, once hybridized with cellulose nanofibers, might be a plausible solution for the incorporation and storage of gases. Such an idea was enhanced by the work of Shah and Imae<sup>98</sup> who reported on the utilisation of 2,2,6,6-tetramethylpiperidine-1-oxyl radical cellulose nanofibers (TOCNF) modified with anion and cation-exchange organoclays, *viz.* hydrotalcite, laponite and sericite. The order of the CO<sub>2</sub> storage ranked among the clays applied is as follows: laponite > sericite > hydrotalcite, with a maximum CO<sub>2</sub> uptake for the laponite-based hybrid material of 24 mg CO<sub>2</sub> per g TOCNF. Hu *et al.*<sup>99</sup> reported on another kind of hierarchical porous N-doped carbon from cellulose in an effective strategy to be utilised as a supercapacitor and in CO<sub>2</sub> capture applications (Fig. 5). The application of such a method emerged from the use of a dissolving-gelling process followed by carbonization in an NH<sub>3</sub> atmosphere, which enhanced the production of both macro- and micropores. The synthesized aerogels had a high adsorption capacity of 4.99 mmol CO<sub>2</sub> per g sorbent which was much higher than those in other porous carbon materials studies as reported accordingly.

ILs and cellulose acetate (CAct),<sup>100</sup> another type of biodegradable polymer as the parent macromolecule, were also exploited for the purposes of CO<sub>2</sub> capturing and separation. Zhang and co-workers<sup>101</sup> reported very recently on the introduction of an ether-functionalized pyridinium-based ionic liquid ([E<sub>n</sub>Py][NTf<sub>2</sub>]/CAct) which was fabricated into





A further recommendation is to find universal protocols to capture CO<sub>2</sub> in terms of gas uptake measuring conditions (volumetric vs. gravimetric), as this may hinder a fair comparison among sorbents.<sup>29</sup> Also, modification/functionalisation of the naturally-occurring polymers might provide better reactivities and performance characteristics.

## Conflicts of interest

There are no conflicts to declare.

## Acknowledgements

AFE acknowledges research support from the Deanship of Scientific Research at the Hashemite University, Jordan.

## Notes and references

- 1 E. S. Poloczanska, C. J. Brown, W. J. Sydeman, W. Kiessling, D. S. Schoeman, P. J. Moore, K. Brander, J. F. Bruno, L. B. Buckley, M. T. Burrows, C. M. Duarte, B. S. Halpern, J. Holding, C. V. Kappel, M. I. O'Connor, J. M. Pandolfi, C. Parmesan, F. Schwing, S. A. Thompson and A. J. Richardson, *Nat. Clim. Change*, 2013, **3**, 919–925.
- 2 I. Nagelkerken and S. D. Connell, *Proc. Natl. Acad. Sci. U. S. A.*, 2015, **112**, 13272–13277.
- 3 A. W. R. Seddon, M. Macias-Fauria, P. R. Long, D. Benz and K. J. Willis, *Nature*, 2016, **531**, 229–232.
- 4 UNFCCC, Adoption of the Paris Agreement., Report No. FCCC/CP/2015/L.9/Rev.1, <http://unfccc.int/resource/docs/2015/cop21/eng/l09r01.pdf>.
- 5 P. Fragkos, N. Tasios, L. Paroussos, P. Capros and S. Tsani, *Energy Policy*, 2017, **100**, 216–226.
- 6 D. G. Victor, K. Akimoto, Y. Kaya, M. Yamaguchi, D. Cullenward and C. Hepburn, *Nature*, 2017, **548**, 25–27.
- 7 J. Rogelj, M. den Elzen, N. Höhne, T. Fransen, H. Fekete, H. Winkler, R. Schaeffer, F. Sha, K. Riahi and M. Meinshausen, *Nature*, 2016, **534**, 631–639.
- 8 S. I. Seneviratne, M. G. Donat, A. J. Pitman, R. Knutti and R. L. Wilby, *Nature*, 2016, **529**, 477–483.
- 9 L. Bretschger, *Environ. Econ. Pol. Stud.*, 2017, **19**, 1–14.
- 10 D. M. D'Alessandro, B. Smit and J. R. Long, *Angew. Chem., Int. Ed.*, 2010, **49**, 6058–6082.
- 11 J.-S. M. Lee, G. Rochelle, P. Styring, P. Fennell, G. Wilson, M. Trusler, P. Clough, J. Blamey, M. Dunstan, N. MacDowell, S. Lyth, J. Yao, T. Hills, M. Gazzani, P. Brandl, R. Anantharaman, S. Brandani, J. Stolaroff, M. Mazzotti, G. Maitland, C. Muller, G. Dowson, J. Gibbins, R. Ocone, K. Sedransk Campbell, M. Erans, L. Zheng, D. Sutter, A. Armutlulu and B. Smit, *Faraday Discuss.*, 2016, **192**, 125–151.
- 12 H. A. Patel, J. Byun and C. T. Yavuz, *ChemSusChem*, 2017, **10**, 1303–1317.
- 13 P. T. Anastas and M. M. Kirchhoff, *Acc. Chem. Res.*, 2002, **35**, 686–694.
- 14 M. Poliakoff, J. M. Fitzpatrick, T. R. Farren and P. T. Anastas, *Science*, 2002, **297**, 807–810.
- 15 P. Anastas and N. Eghbali, *Chem. Soc. Rev.*, 2010, **39**, 301–312.
- 16 E. D. Bates, R. D. Mayton, I. Ntai and J. H. Davis, *J. Am. Chem. Soc.*, 2002, **124**, 926–927.
- 17 D. J. Heldebrant, P. K. Koech, M. T. C. Ang, C. Liang, J. E. Rainbolt, C. R. Yonker and P. G. Jessop, *Green Chem.*, 2010, **12**, 713–721.
- 18 A. Gandini, *Macromolecules*, 2008, **41**, 9491–9504.
- 19 A. Gandini, T. M. Lacerda, A. J. F. Carvalho and E. Trovatti, *Chem. Rev.*, 2016, **116**, 1637–1669.
- 20 D. K. Schneiderman and M. A. Hillmyer, *Macromolecules*, 2017, **50**, 3733–3749.
- 21 B. Medronho, A. Romano, M. G. Miguel, L. Stigsson and B. Lindman, *Cellulose*, 2012, **19**, 581–587.
- 22 M. Rinaudo, *Prog. Polym. Sci.*, 2006, **31**, 603–632.
- 23 D. G. Ramirez-Wong, M. Ramirez-Cardona, R. J. Sanchez-Leija, A. Rugerio, R. A. Mauricio-Sanchez, M. A. Hernandez-Landaverde, A. Carranza, J. A. Pojman, A. M. Garay-Tapia, E. Prokhorov, J. D. Mota-Morales and G. Luna-Barcenas, *Green Chem.*, 2016, **18**, 4303–4311.
- 24 H. Mahmood, M. Moniruzzaman, S. Yusup and T. Welton, *Green Chem.*, 2017, **19**, 2051–2075.
- 25 R. P. Swatloski, S. K. Spear, J. D. Holbrey and R. D. Rogers, *J. Am. Chem. Soc.*, 2002, **124**, 4974–4975.
- 26 P. Styring, in *Carbon Dioxide Utilisation*, Elsevier, Amsterdam, 2015, pp. 19–32.
- 27 R. W. Flaig, T. M. Osborn Popp, A. M. Fracaroli, E. A. Kapustin, M. J. Kalmutzki, R. M. Altamimi, F. Fathieh, J. A. Reimer and O. M. Yaghi, *J. Am. Chem. Soc.*, 2017, **139**, 12125–12128.
- 28 A. F. Eftaiha, A. K. Qaroush, K. I. Assaf, F. Alsubhani, T. Markus Pehl, C. Troll and M. I. El-Barghouthi, *New J. Chem.*, 2017, **41**, 11941–11947.
- 29 A. K. Qaroush, D. A. Castillo-Molina, C. Troll, M. A. Abu-Daibes, H. M. Alsayouri, A. S. Abu-Surrah and B. Rieger, *ChemSusChem*, 2015, **8**, 1618–1626.
- 30 P. V. Kortunov, M. Siskin, L. S. Baugh and D. C. Calabro, *Energy Fuels*, 2015, **29**, 5940–5966.
- 31 P. V. Kortunov, M. Siskin, L. S. Baugh and D. C. Calabro, *Energy Fuels*, 2015, **29**, 5919–5939.
- 32 F. Inagaki, C. Matsumoto, T. Iwata and C. Mukai, *J. Am. Chem. Soc.*, 2017, **139**, 4639–4642.
- 33 Y. Park, K.-Y. A. Lin, A.-H. A. Park and C. Petit, *Frontiers in Energy Research*, 2015, **3**, 42.
- 34 Sigma-Aldrich Co., Ethanolamine  $\geq 98\%$ , <http://www.sigmaaldrich.com/catalog/product/sial/e9508?lang=en&region=JO>, accessed on 15.Oct.2017.
- 35 Alfa Aesar™, Ethanolamine, 98+%, <https://www.fishersci.com/shop/products/ethanolamine-98-3/p-7081646#?keyword=Monoethanolamine>, accessed on 15.Oct.2017.
- 36 S. Seo, M. Quiroz-Guzman, M. A. DeSilva, T. B. Lee, Y. Huang, B. F. Goodrich, W. F. Schneider and J. F. Brennecke, *J. Phys. Chem. B*, 2014, **118**, 5740–5751.
- 37 V. V. Chaban, *RSC Adv.*, 2016, **6**, 8906–8912.



- 38 S. Zeng, X. Zhang, L. Bai, X. Zhang, H. Wang, J. Wang, D. Bao, M. Li, X. Liu and S. Zhang, *Chem. Rev.*, 2017, **117**, 9625–9673.
- 39 P. G. Jessop, D. J. Heldebrant, X. Li, C. A. Eckert and C. L. Liotta, *Nature*, 2005, **436**, 1102.
- 40 P. Pollet, C. A. Eckert and C. L. Liotta, *Chem. Sci.*, 2011, **2**, 609–614.
- 41 J. J. Gassensmith, H. Furukawa, R. A. Smaldone, R. S. Forgan, Y. Y. Botros, O. M. Yaghi and J. F. Stoddart, *J. Am. Chem. Soc.*, 2011, **133**, 15312–15315.
- 42 D. Wu, J. J. Gassensmith, D. Gouvêa, S. Ushakov, J. F. Stoddart and A. Navrotsky, *J. Am. Chem. Soc.*, 2013, **135**, 6790–6793.
- 43 J. J. Gassensmith, J. Y. Kim, J. M. Holcroft, O. K. Farha, J. F. Stoddart, J. T. Hupp and N. C. Jeong, *J. Am. Chem. Soc.*, 2014, **136**, 8277–8282.
- 44 H. A. Patel, T. Islamoglu, Z. Liu, S. K. M. Nalluri, A. Samanta, O. Anamimoghadam, C. D. Malliakas, O. K. Farha and J. F. Stoddart, *J. Am. Chem. Soc.*, 2017, **139**, 11020–11023.
- 45 R. Rajamanickam, H. Kim and J.-W. Park, *Sci. Rep.*, 2015, **5**, 10688.
- 46 A. K. Qaroush, K. I. Assaf, A. Al-Khateeb, F. Alsoubani, E. Nabih, C. Troll, B. Rieger and A. F. Eftaiha, *Energy Fuels*, 2017, **31**, 8407–8414.
- 47 K. I. Assaf, A. K. Qaroush and A. F. Eftaiha, *Phys. Chem. Chem. Phys.*, 2017, **19**, 15403–15411.
- 48 A. C. O'Sullivan, *Cellulose*, 1997, **4**, 173–207.
- 49 I. Siró and D. Plackett, *Cellulose*, 2010, **17**, 459–494.
- 50 J. Cai and L. Zhang, *Macromol. Biosci.*, 2005, **5**, 539–548.
- 51 C. L. McCormick, P. A. Callais and B. H. Hutchinson, *Macromolecules*, 1985, **18**, 2394–2401.
- 52 H. Qi, C. Chang and L. Zhang, *Cellulose*, 2008, **15**, 779–787.
- 53 S. Zhu, Y. Wu, Q. Chen, Z. Yu, C. Wang, S. Jin, Y. Ding and G. Wu, *Green Chem.*, 2006, **8**, 325–327.
- 54 M. Abe, Y. Fukaya and H. Ohno, *Chem. Commun.*, 2012, **48**, 1808–1810.
- 55 D. L. Minnick and A. M. Scurto, *Chem. Commun.*, 2015, **51**, 12649–12652.
- 56 X. Sun, Y. Chi and T. Mu, *Green Chem.*, 2014, **16**, 2736–2744.
- 57 Q. Zhang, M. Benoit, K. De Oliveira Vigier, J. Barrault and F. Jérôme, *Chem.–Eur. J.*, 2012, **18**, 1043–1046.
- 58 Q.-P. Liu, X.-D. Hou, N. Li and M.-H. Zong, *Green Chem.*, 2012, **14**, 304–307.
- 59 M. Francisco, A. van den Bruinhorst and M. C. Kroon, *Green Chem.*, 2012, **14**, 2153–2157.
- 60 Q. Zhang, N. S. Oztekin, J. Barrault, K. De Oliveira Vigier and F. Jérôme, *ChemSusChem*, 2013, **6**, 593–596.
- 61 Y. Yang, L. Song, C. Peng, E. Liu and H. Xie, *Green Chem.*, 2015, **17**, 2758–2763.
- 62 J. Wang, Z. Xue, T. Yu, Z. Liu and T. Mu, *Chem.–Asian J.*, 2017, **12**, 1773–1779.
- 63 L. Song, Y. Yang, H. Xie and E. Liu, *ChemSusChem*, 2015, **8**, 3217–3221.
- 64 J. Wang, Z. Xue, C. Yan, Z. Li and T. Mu, *Phys. Chem. Chem. Phys.*, 2016, **18**, 32772–32779.
- 65 M. Gunnarsson, H. Theliander and M. Hasani, *Cellulose*, 2017, **24**, 2427–2436.
- 66 S. Y. Oh, D. I. Yoo, Y. Shin and G. Seo, *Carbohydr. Res.*, 2005, **340**, 417–428.
- 67 H. Xie, X. Yu, Y. Yang and Z. K. Zhao, *Green Chem.*, 2014, **16**, 2422–2427.
- 68 P. Nanta, W. Skolpap, K. Kasemwong and Y. Shimoyama, *J. Supercrit. Fluids*, 2017, **130**, 84–90.
- 69 E. M. M. D. Valle, *Process Biochem.*, 2004, **39**, 1033–1046.
- 70 Z. Liu, S. K. M. Nalluri and J. F. Stoddart, *Chem. Soc. Rev.*, 2017, **46**, 2459–2478.
- 71 R. A. Smaldone, R. S. Forgan, H. Furukawa, J. J. Gassensmith, A. M. Z. Slawin, O. M. Yaghi and J. F. Stoddart, *Angew. Chem., Int. Ed.*, 2010, **49**, 8630–8634.
- 72 Note: Using diisopropyl ether (*i*Pr<sub>2</sub>O) instead of MeOH resulted in the formation of a metal coordination framework (MCF). For more details please see the following reference: J. J. Gassensmith, R. A. Smaldone, R. S. Forgan, C. E. Wilmer, D. B. Cordes, Y. Y. Botros, A. M. Z. Slawin, R. Q. Snurr and J. F. Stoddart, *Org. Lett.*, 2012, **14**, 1460–1463.
- 73 R. S. Forgan, R. A. Smaldone, J. J. Gassensmith, H. Furukawa, D. B. Cordes, Q. Li, C. E. Wilmer, Y. Y. Botros, R. Q. Snurr, A. M. Z. Slawin and J. F. Stoddart, *J. Am. Chem. Soc.*, 2012, **134**, 406–417.
- 74 Note: Neither  $\gamma$ -cyclodextrin nor crushed CD-MOF-2 (an amorphous material as obtained from XRD measurements) were able to absorb CO<sub>2</sub>.
- 75 D. L. Sivasdas, K. P. Vijayalakshmi, R. Rajeev, K. Prabhakaran and K. N. Ninan, *RSC Adv.*, 2013, **3**, 24041–24045.
- 76 Y.-C. Zhao, L. Zhao, L.-J. Mao and B.-H. Han, *J Mater Chem A*, 2013, **1**, 9456–9461.
- 77 T. Guo, A. H. Bedane, Y. Pan, B. Shirani, H. Xiao and M. Eić, *Energy Fuels*, 2017, **31**, 4186–4192.
- 78 G. V. S. M. Carrera, N. Jordao, L. C. Branco and M. Nunes da Ponte, *Faraday Discuss.*, 2015, **183**, 429–444.
- 79 P. R. Austin, in *Chitin, Chitosan, and Related Enzymes*, Academic Press, 1984, pp. 227–237.
- 80 P. R. Sivashankari and M. Prabakaran, in *Chitosan Based Biomaterials Volume 1*, Woodhead Publishing, 2017, pp. 117–133.
- 81 H. Xie, S. Zhang and S. Li, *Green Chem.*, 2006, **8**, 630–633.
- 82 X. Sun, C. Huang, Z. Xue and T. Mu, *Energy Fuels*, 2015, **29**, 1923–1930.
- 83 X. Sun, Z. Xue and T. Mu, *Green Chem.*, 2014, **16**, 2102–2106.
- 84 G. E. Romanos, P. S. Schulz, M. Bahlmann, P. Wasserscheid, A. Sapolidis, F. K. Katsaros, C. P. Athanasekou, K. Beltsios and N. K. Kanellopoulos, *J. Phys. Chem. C*, 2014, **118**, 24437–24451.
- 85 K. Pohako-Esko, M. Bahlmann, P. S. Schulz and P. Wasserscheid, *Ind. Eng. Chem. Res.*, 2016, **55**, 7052–7059.
- 86 J. Fujiki and K. Yogo, *Chem. Lett.*, 2013, **42**, 1484–1486.
- 87 J. Fujiki and K. Yogo, *Energy Fuels*, 2014, **28**, 6467–6474.
- 88 A. F. Eftaiha, F. Alsoubani, K. I. Assaf, W. M. Nau, C. Troll and A. K. Qaroush, *RSC Adv.*, 2016, **6**, 22090–22093.



- 89 A. F. Eftaiha, F. Alsoubani, K. I. Assaf, C. Troll, B. Rieger, A. H. Khaled and A. K. Qaroush, *Carbohydr. Polym.*, 2016, **152**, 163–169.
- 90 A. K. Qaroush, K. I. Assaf, S. K. Bardaweel, A. Al-Khateeb, F. Alsoubani, E. Al-Ramahi, M. Masri, T. Bruck, C. Troll, B. Rieger and A. F. Eftaiha, *Green Chem.*, 2017, **19**, 4305–4314.
- 91 C. Gebald, J. A. Wurzbacher, P. Tingaut, T. Zimmermann and A. Steinfeld, *Environ. Sci. Technol.*, 2011, **45**, 9101–9108.
- 92 C. Gebald, J. A. Wurzbacher, P. Tingaut and A. Steinfeld, *Environ. Sci. Technol.*, 2013, **47**, 10063–10070.
- 93 M. Sevilla and A. B. Fuertes, *Energy Environ. Sci.*, 2011, **4**, 1765–1771.
- 94 D. M. Pacheco, J. R. Johnson and W. J. Koros, *Ind. Eng. Chem. Res.*, 2012, **51**, 503–514.
- 95 F. S. Li, R. P. Lively, J. S. Lee and W. J. Koros, *Ind. Eng. Chem. Res.*, 2013, **52**, 8928–8935.
- 96 Y.-J. Heo and S.-J. Park, *Energy*, 2015, **91**, 142–150.
- 97 F. L. Bernard, D. M. Rodrigues, B. B. Polesso, A. J. Donato, M. Seferin, V. V. Chaban, F. D. Vecchia and S. Einloft, *Fuel Process. Technol.*, 2016, **149**, 131–138.
- 98 K. J. Shah and T. Imae, *Biomacromolecules*, 2016, **17**, 1653–1661.
- 99 Y. Hu, X. Tong, H. Zhuo, L. Zhong, X. Peng, S. Wang and R. Sun, *RSC Adv.*, 2016, **6**, 15788–15795.
- 100 L. Jiang and G. Hinrichsen, *Angew. Makromol. Chem.*, 1997, **253**, 193–200.
- 101 J. Deng, L. Bai, S. Zeng, X. Zhang, Y. Nie, L. Deng and S. Zhang, *RSC Adv.*, 2016, **6**, 45184–45192.
- 102 B. Lam, M. Wei, L. Zhu, S. Luo, R. Guo, A. Morisato, P. Alexandridis and H. Lin, *Polymer*, 2016, **89**, 1–11.
- 103 L. Ansaloni, J. Salas-Gay, S. Ligi and M. G. Baschetti, *J. Membr. Sci.*, 2017, **522**, 216–225.
- 104 R. S. Dassanayake, C. Gunathilake, A. C. Dassanayake, N. Abidi and M. Jaroniec, *J Mater Chem A*, 2017, **5**, 7462–7473.
- 105 D. G. Reed, G. R. M. Dowson and P. Styring, *Frontiers in Energy Research*, 2017, **5**, 13.
- 106 Business Opportunities in Carbon Capture and Utilisation, 56, 2017, [http://www.climeworks.com/wp-content/uploads/2017/05/2017\\_03\\_30\\_Carbon-Captur-Journal\\_Climeworks-captures-CO2-directly-from-the-atmosphere.pdf](http://www.climeworks.com/wp-content/uploads/2017/05/2017_03_30_Carbon-Captur-Journal_Climeworks-captures-CO2-directly-from-the-atmosphere.pdf).

